J Mater Sci (2020) 55:6051–6064

Materials for life sciences

Impact of a bioactive drug coating on the biocompatibility of magnesium alloys

Quan Liang[1], Ge Shuping[1,2,*], Liu Chenyu[1], Jia Dongyu[3], Wang Guixue[2], and Yin Tieying[2]

[1] School of Chemistry and Chemical Engineering, Chongqing University of Technology, Chongqing 400054, People's Republic of China

[2] Key Laboratory of Biorheological Science and Technology, Chongqing University, Chongqing, China

[3] Department of Biology, Georgia Southern University, Statesboro, GA, USA

Received: 22 October 2019
Accepted: 15 January 2020
Published online: 4 February 2020

ABSTRACT

Magnesium alloys are promising materials for biodegradable vascular stents because of their good biocompatibility and physical properties. The poly-β-hydroxybutyrate (PHB) coating with vascular endothelial growth factor and heparin was prepared on the surface of WE magnesium alloys by layer-by-layer self-assembly technique. In this study, the effects of magnesium alloys with bioactive drug coating on human umbilical vein endothelial cells (HUVECs) and blood compatibility were investigated. The results showed that magnesium alloys with bioactive drug coating could decrease platelet adhesion, platelet activation, hemolysis rate, fibrinogen adsorption and increase activated partial thromboplastin time, prothrombin time, dynamic clotting of magnesium alloys. In addition, magnesium alloys with bioactive drug coating did not alter cytoskeleton morphological features of HUVECs, promoted cell adhesion and cell growth, and inhibited cell apoptosis. Therefore, the magnesium alloys with bioactive drug coating can be considered as potential and degradable biomaterials for vascular stents.

Introduction

In recent years, magnesium alloys have been considered as potential and biodegradable biomaterials in medical implant materials field due to their excellent biocompatibility and mechanical properties [1–6]. However, the degradation of magnesium alloys in solution limits their application as vascular stent materials [7]. Hence, it is of great significance to control the degradation rate of magnesium alloys for biomedical application.

Researchers have tried to address the degradation of magnesium alloys through microstructural and surface modification strategies [8]. As for surface modification, protective coating is widely applied to mitigating the degradation of magnesium alloys [9]. In contrast to inorganic coatings, biodegradable polymeric coatings have better properties [10]. As a

Address correspondence to E-mail: geshupingcqu@163.com

https://doi.org/10.1007/s10853-020-04365-4

naturally biodegradable polymeric material, poly-β-hydroxybutyrate (PHB) belongs to the family of poly-β-hydroxyalkanoates and has been applied as biodegradable and biocompatible plastics. PHB can facilitate cell adhesion and has good biodegradability and biocompatibility [11–13]. Using PHB as the coating basement can control the degradation rate of magnesium alloys [14, 15]. Therefore, this study chose PHB as the base coating material to control the degradation of magnesium alloys by adjusting the thickness and the number of layers of PHB coating. In addition, as for biodegradable vascular stent materials, they are required to accelerate endothelialization and ensure the effect of anti-thrombosis. In order to meet the required properties of vascular stent materials, LbL self-assembly technology was proposed to coat materials with drug and construct nanoscale films on the surface of materials [16].

The purpose of this study was to investigate the blood compatibility and cell compatibility of magnesium alloys with bioactive drug coating. Firstly, the PHB coating was prepared on the surface of naked magnesium alloys. Then, the PHB coating was ammoniated by 1,6-hexanediamine, and the surface coating of the material was assembled by LbL self-assembly technique to construct degradation resistance and bioactive drug coating. Next, blood compatibility and cell morphology, cell adhesion, cell apoptosis and the other properties were used to determine the biocompatibility of samples. The composite coating provides a new surface modification strategy for the bioactive coating construction of biodegradable magnesium alloys.

Materials and methods

Materials

Magnesium alloys used in this study were Mg-4.1Y-2.8Nd-0.2Zn-0.4Zr alloys (4.1%Y, 2.8%Nd, 0.2%Zn, 0.4% Zr and Mg balance; tensile strength: 250 MPa; yield strength: 180 MPa; elongation: 4%). Chloroform, acetone, ethanol and 1,6-hexanediamine/n-propanol were purchased from Chuandong Chemical, Chongqing, China. Acid Orange7 (AO) was purchased from Yousuo Chemical Technology, China; Phalloidin kit and poly-β-hydroxybutyrate (PHB) powder were purchased from Sigma-Aldrich, USA. AO-EB (acridine orange–ethidium bromide) double dyeing kits were purchased from Solarbio, Beijing, China. The APTT kits, PT kits, phosphate-buffered saline (PBS) and heparin were acquired from Jiancheng Bioengineering, Nanjing, China. The Roswell Park Memorial Institute (RPMI) 1640 medium and fetal bovine serum (FBS) were obtained from Hyclone Company, China. The 3,3′,5,5′-Tetramethylbenzidine (TMB) was purchased from horseradish peroxidase (HRP) YuanyeBio, Shanghai, China. The VEGF, goat anti-human antibody (IgG) and antibody protective solution were purchased from Proteintech, Wuhan, China. HUVECs were from EA.hy926 cell strain, which was purchased from Cell Bank of Chinese Academy of Sciences, Shanghai, China.

The extracts of blood compatibility test were obtained by immersing samples in physiological saline solution at a ratio of 3 cm^2/mL and incubated in water bath for 24 h at 37 °C.

The extracts of cell compatibility test were obtained by placing the samples into leaching medium at a ratio of 1.25 cm^2/mL for 72 h in an incubator containing 5% CO_2, at 37 °C. The extraction medium was diluted to 25% and 50% solution with RPMI1640 medium supplemented with 10% FBS and stored at 4 °C.

Preparation of coating

The magnesium alloys were cut into pieces of 8 mm × 2 mm; then, the surface of materials was polished with metallographic sandpaper of 400#,800#,1000#, 2000# and 4000#. PHB solution was prepared by dissolving PHB powder in chloroform at 60 °C for 2 h. Then, the materials were cleaned ultrasonically in acetone, absolute ethanol and ultra-pure water for 10 min (samples were immersed in liquid) before drying at room temperature. To construct PHB film on magnesium alloys, magnesium alloys were incubated in 0.5 g/L of PHB solution. The primary amino group can react with the ester group –COO– of PHB by a nucleophilic substitution under certain conditions. Once one of the amine groups of hexamethylenediamine (HD) was bound with main molecular chain of PHB, another amine group at the distal end would maintain free with a high probability [17]. Then, the samples containing PHB coating were put into the 1,6-hexanediamine/n-propanol solution (6 mg/mL, soluble in n-propanol), heated in water bath at 40 °C for 30 min and rinsed with ultra-pure water to remove residual

hexanediamine. The ammoniated magnesium alloys were dried in a vacuum oven at 30 °C until the surface was positively charged with constant weight. The concentration of heparin in ultra-pure water was 3 mg/mL, pH value was 4.2, and the concentration of VEGF in PBS was 100 mg/mL. To prepare magnesium alloys with bioactive drug coating, heparin was negatively charged by adjusting the pH value of the solution. In the same way, VEGF is positively charged. The process was repeated for three times until six layers of drug coating were obtained on the surface of materials by LbL self-assembly method (Fig. 1).

Cell culture

HUVECs were cultured in RPMI1640 medium supplemented with 10% FBS in an incubator containing 5% CO_2 at 37 °C.

Preparation of PRP and PPP

Healthy human blood from a volunteer was mixed with 3.8% sodium citrate at a ratio of 9:1 and centrifuged for 10 min [18, 19]. The supernatant was platelet-rich plasma (PRP), and precipitate was platelet-poor plasma (PPP). The experimental protocols were approved by Ethics Committee of Chongqing University of Technology and based on ISO 10993-4:2017.

Quantification of the amine of samples

The AO/NaOH solution (1×10^{-3} mol/L) was diluted with NaOH to different concentration gradients (1×10^{-6} mol/L, 2×10^{-6} mol/L, 3×10^{-6} mol/L, 5×10^{-6} mol/L, 8×10^{-6} mol/L and 10×10^{-6} mol/L). The absorbance was recorded at 492 nm by spectrophotometer, and the absorbance–concentration standard curve was established.

The samples with PHB coating, ammoniated coating and bioactive drug coating were immersed in 5×10^{-4} mol/L AO/HCl solution (pH = 3) and stirred for 5 h at 37 °C to obtain amino/AO ionic compound on the surface of the samples. After washing the residual AO, the 1×10^{-3} mol/L NaOH solution was used to unload the AO in amino/AO ionic compound. Finally, the density of amine was quantified by the absorbance–concentration standard curve.

Platelet adhesion

The magnesium alloys with PHB coating, ammoniated coating and bioactive drug coating were washed with physiological saline and equilibrated in PBS buffer for 2 h, respectively. Then, the samples were placed into PRP and maintained at 37 °C for 1 h, and rinsed slightly with PBS buffer. The samples were treated with 2.5% glutaraldehyde solution (preserved at 4 °C in advance) for 1.5 h, and dehydrated with a series of graded alcohol solutions (30%, 50%, 70%, 80%, 90%, 95% and 100%) for 30 min each time, then frozen for 24 h. After the gold spraying, the surface morphology was observed by scanning electron microscope (SEM, FEI Nova 400).

Platelet activation

The magnesium alloys with PHB coating, ammoniated coating and bioactive drug coating were immersed in PRP, respectively, and incubated at 37 °C for 2 h. After removing the plasma, the samples were blocked with 5% sheep serum for 15 min, repeating the procedure twice. Then, removing the surface fluid, the samples with antibody working solution were incubated for 2 h and washed with PBS for 5 min, repeating the procedure for three times. Later, the surface liquid of the sample was removed and incubated in peroxidase-labelled IgG solution for 1 h. After draining the surface liquid of the sample, the TMB was added and reacted in the dark for 30 min. Then, adding the same amount of concentrated sulphuric acid, the colour reaction was terminated, and the absorbance was recorded at 450 nm.

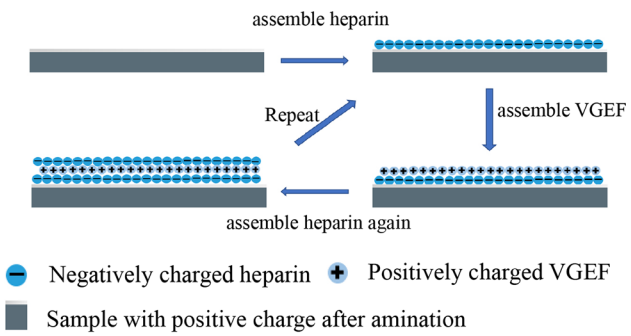

Figure 1 Schematic of LbL self-assembly technique.

Hemolysis rate

The whole blood containing anti-coagulation was diluted with physiological saline at a ratio of 4:5. Then, the extracts of magnesium alloys with PHB coating, ammoniated coating and bioactive drug coating were added into the diluted blood, respectively, and placed in a water bath at 37 °C for 60 min. Physiological saline with fresh human blood was used as negative controls. The deionized water with fresh human blood served as a positive control. Then, each tube was centrifuged at 3000 rpm/min for 15 min. Finally, the absorbance of supernatant was detected at 545 nm. The process was repeated for five times. The hemolysis rate of the samples was calculated using the following formula:

$$\text{Hemolysis rate}\,(\%) = (D_t - D_{\text{nc}}) / (D_{\text{pc}} - D_{\text{nc}}) \times 100\%$$

where D_t is the absorbance of the samples, D_{nc} is referred to as the absorbance of the negative control, and D_{pc} is the absorbance of the positive control.

Fibrinogen adsorption

The magnesium alloys with PHB coating, ammoniated coating and bioactive drug coating were placed in PPP, respectively, and incubated for 2 h at 37 °C, subsequently washed three times with PBS blocking solution in 5% lamb serum. The materials were taken out and added into HRP-coated goat anti-human solution at 37 °C and incubated in PBS solution. After the removal of surface liquid, the samples were put into new holes, and the developer TMB was added. After reacting for 5–10 min, the colour reaction was terminated with sulphuric acid. The absorbance was recorded at 450 nm.

PT and APTT

The PT and APTT were detected according to the manual instruction of kits provided by Jiancheng Bioengineering. The mixture of PPP and extracts of magnesium alloys with PHB coating, ammoniated coating and bioactive drug coating were incubated at 37 °C for 3 min, respectively. Then, the mixture was mixed immediately with preheated prothrombin reagent and $CaCl_2$ solution, respectively. Finally, the plasma coagulation time was recorded by a coagulometer.

Dynamic clotting time

The fresh blood was added to the surface of magnesium alloys with PHB coating, ammoniated coating and bioactive drug coating and incubated at 37 °C for 5, 15, 20, 25, 30, 35, 40, 45, 50, 55 and 60 min, respectively. Then, the samples were transferred into a beaker containing 15 mL of ultra-pure water and rinsed gently. After shaking, a spectrophotometer was used to determine the absorbance of the solution at 450 nm. The clotting time curve was drawn by the relationship between the absorbance and time.

Cell morphology

HUVECs (1×10^5/mL, 0.5 mL) were cultured with 25%, 50% and 100% concentrations of the cell compatibility extracts of different coating samples for 24 h, respectively, and washed with PBS for 3 min, repeating three times. Later, cells were fixed with 2.5% glutaraldehyde for 2 h and then washed with PBS for 5 min, repeating three times. Then, the samples were soaked into 30%, 50%, 70%, 80%, 90%, 100% ethanol for 10 min, respectively. After dehydration, the samples were dried in a vacuum drying oven for at least 12 h. After gold spraying, the cells morphology was observed by SEM.

Cytoskeleton

Firstly, HUVECs (1×10^5/mL) were seeded in 24-well plates (0.5 mL per well) and placed in a CO_2 incubator for 24 h. After culturing HUVECs with 25%, 50% and 100% concentrations of the cell compatibility extracts of different coating samples, respectively, cells were fixed with 4% polyformaldehyde solution for 20 min at room temperature and washed with PBS for 3 min, repeating three times. Then, HUVECs were permeabilized with 0.1% Triton X-100 at room temperature for 10 min. The experimental operation was based on the instruction manual of Phalloidin kit provided by Sigma-Aldrich. The Actin-Tracker Green (from Phalloidin kit) was diluted with PBS containing 1% BSA at ratio of 1:40. After dropping 200 μL of the Actin-Tracker Green staining solution to the cells, they were incubated at 37 °C for 60 min in dark and washed with PBS for 3 min, repeating the process for four times. Then, the cells were observed directly by a laser confocal scanning microscopy (Leica, GER). Subsequently, cells were

stained with DAPI and washed with PBS for 3 min, repeating for three times. Finally, the cytoskeleton was observed. The cell aspect ratio, cell nucleus aspect ratio, cell area and fluorescence intensity were calculated using ImageJ software.

AO/EB staining

HUVECs (1×10^5/mL, 0.5 mL) were cultured with 25%, 50% and 100% concentrations of the cell compatibility extracts of different coating samples for 24 h, respectively, and washed with PBS, repeating for three times. AO/EB staining was carried out according to the manual instruction provided by the manufacturer. The cells were observed by a laser confocal scanning microscopy, in which the dead cells were appeared in red colour and the living cells were appeared in green colour. The green cells and red cells were calculated by ImageJ software.

Statistical analysis

ImageJ software was used to analyse and calculate cells. All the data graphs were drawn by OriginPro2018, and statistical Program for Social Sciences (SPSS, version 22.0) was used for statistical analysis. Comparisons among group means were determined by one-way analysis of variance (ANOVA), and multiple comparisons between two means were conducted by Duncan's multiple range method. The $p < 0.05$ was considered statistically significant, * for $p < 0.05$, ** for $p < 0.01$ and *** for $p < 0.001$.

Results and discussion

Density of amine

The quantification of amine concentration is shown in Fig. 2. The samples after amination (ammoniated coating and bioactive drug coating) had obviously higher amine density than the original PHB coating. The amine density of bioactive drug coating was just little lower than ammoniated coating, which was probably caused by the damage of HCl and NaOH in the process of ionic compound formation or unloading the AO. Otherwise, surface amination can achieve positively charged surface under physiological conditions and enable the biomaterial surface to interact electrostatically with the negatively charged cell surface for increasing the properties of cell and blood adhesion [20, 21].

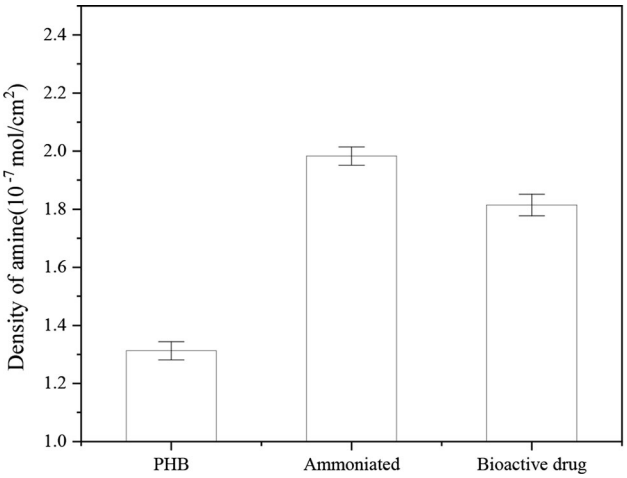

Figure 2 Amine density of different samples. (i) PHB: magnesium alloys with PHB coating; (ii) ammoniated: magnesium alloys with ammoniated coating; and (iii) bioactive drug: magnesium alloys with bioactive drug coating.

Platelet adhesion

As shown in Fig. 3a, b, the number of adherent platelets on the surface of different samples showed obvious differences. The number of adherent platelets was counted in five randomly selected areas. It showed that the ammoniated samples had significantly more adherent platelets than samples with PHB coating and samples with bioactive drug coating. The latter showed few adhered platelets on the surface of magnesium alloys with bioactive drug coating.

Platelet adhesion is one of the important elements for the thrombosis–pathogenesis [22]. The bioactive drug coating could significantly decrease platelet adhesion and improve hemocompatibility. Heparin could reduce the thrombosis [23], which proved that the bioactive drugs were assembled on the ammoniated samples successfully.

Platelet activation

Figure 4 shows that the ability of platelet activation for samples with bioactive drug coating was lower than the other samples, while the ammoniated sample was the highest. The results were consistent with other findings that VEGF particles significantly inhibited platelet adhesion and activation [24]. It

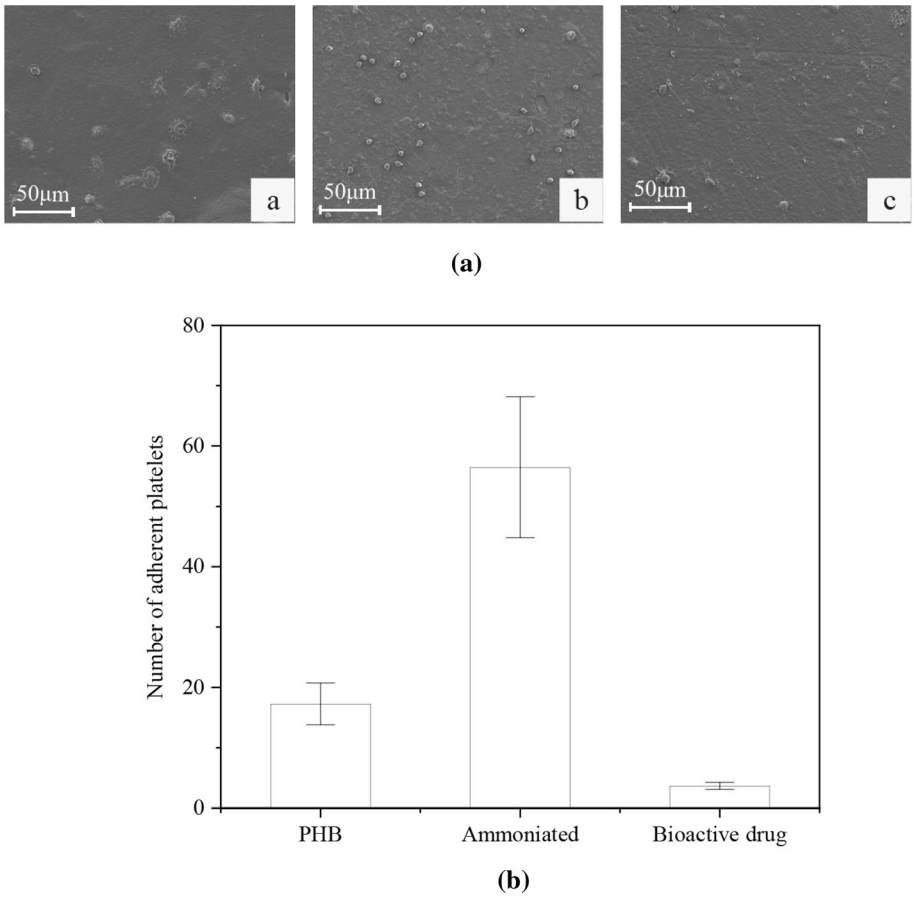

Figure 3 **a** SEM images of platelets adhered to magnesium alloys with different coatings. (i): magnesium alloys with PHB coating, (ii): magnesium alloys with ammoniated coating, and (iii): magnesium alloys with bioactive drug coating. Original magnification: 500 ×. **b** Comparison of platelet adhesion on the surface of magnesium alloys with different coatings. (i) PHB: magnesium alloys with PHB coating; (ii) ammoniated: magnesium alloys with ammoniated coating; and (iii) bioactive drug: magnesium alloys with bioactive drug coating.

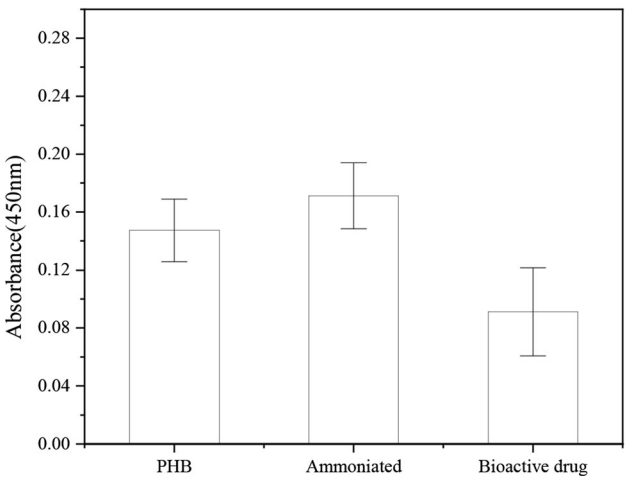

Figure 4 Effect of magnesium alloys with different coatings on platelet activation. (i) PHB: magnesium alloys with PHB coating; (ii) ammoniated: magnesium alloys with ammoniated coating; and (iii) bioactive drug: magnesium alloys with bioactive drug coating.

could be considered that the hexamethylenediamine and positive charge on the surface of ammoniated samples could increase the possibility of thrombus. When VEGF particles assembled on the coating, the samples with bioactive drug coating had better anti-thrombotic performance than other samples.

Hemolysis rate

Figure 5 shows that the hemolysis rate of samples with bioactive drug coating was significantly lower than those of other samples.

Hemolysis rate could serve as an indicator of damage, which might occur during the sample contact with blood [25]. Hemolysis rate can be used in screening tests for medical materials in contact with blood [26]. The ammoniated samples caused great damage to blood cells (the hemolysis rate is 91.64%), while the samples with bioactive drug coating

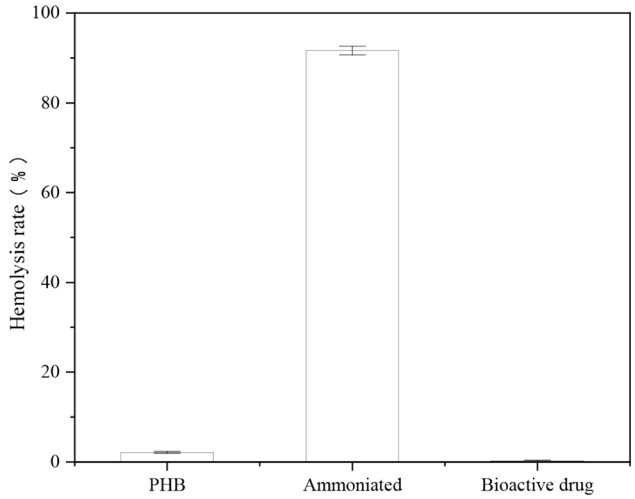

Figure 5 Hemolysis rate of magnesium alloys with different coatings. (i) PHB: magnesium alloys with PHB coating; (ii) ammoniated: magnesium alloys with ammoniated coating; (iii) bioactive drug: magnesium alloys with bioactive drug coating; (iv) positive control: distilled water; and (v) negative control: 0.9% NaCl.

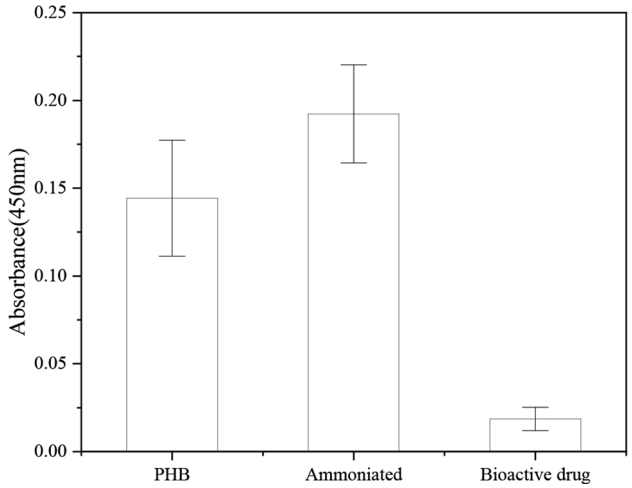

Figure 6 Effect of magnesium alloys with different coatings on fibrinogen absorption. (i) PHB: magnesium alloys with PHB coating; (ii) ammoniated: magnesium alloys with ammoniated coating; and (iii) bioactive drug: magnesium alloys with bioactive drug coating.

showed a low level of hemolysis rate (0.24%). It has been demonstrated that VEGF and heparin modification could improve blood compatibility [24]. In this study, low hemolysis rate of bioactive drug samples might be due to the effects of VEGF and heparin.

Fibrinogen adsorption

The fibrinogen secreted by the liver is present in blood plasma at a concentration of 200–400 mg/dL. It yields monomers that can polymerize into fibrin. As fibrin is a cofactor in platelet aggregation, platelets need fibrinogen to activate aggregation of platelets [27]. Therefore, the fibrinogen absorption can be used to evaluate the blood compatibility of materials [28]. Figure 6 shows that the samples with bioactive drug coating had a lower ability of fibrinogen absorption compared to the samples with PHB coating and ammoniated samples. Thus, the samples with bioactive drug coating had better blood compatibility.

PT and APTT

Figures 7 and 8 show the results of APTT and PT. The samples with bioactive drug coating had longer clotting time than other samples and control group.

The APTT and PT assays were used to evaluate the deficiency or excess of clotting factors [29–33]. They were also adapted to monitor changes in clotting time

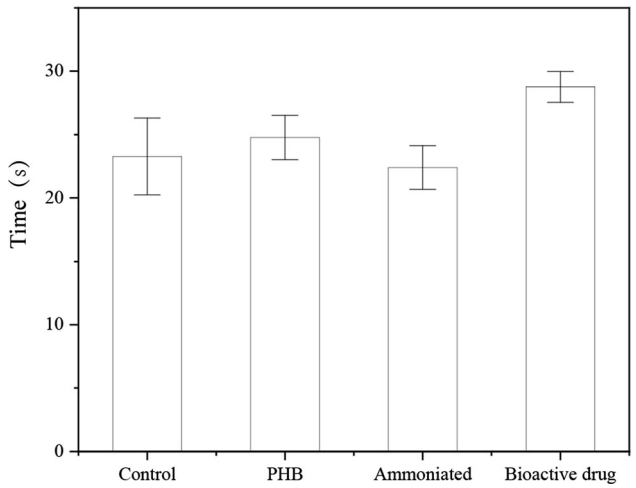

Figure 7 APPT of magnesium alloys with different coatings. (i) PHB: magnesium alloys with PHB coating; (ii) ammoniated: magnesium alloys with ammoniated coating; (iii) bioactive drug: magnesium alloys with bioactive drug coating; and (iv) control: 0.9% NaCl.

by exposing the fresh human blood to biomaterials [34]. Both the PT and APTT of the samples with bioactive drug coating were longer than other samples. In the clinic, heparin has anticoagulant effect [35–38]. As the research shows, the heparin can prolong PT and APTT. It can be inferred that the bioactive drug coating releases heparin into blood, which can decrease the possibility of thrombosis.

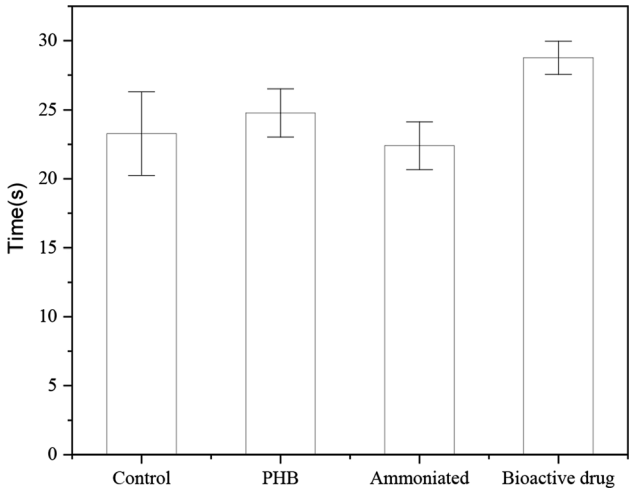

Figure 8 PT of magnesium alloys with different coatings. (i) PHB: magnesium alloys with PHB coating; (ii) ammoniated: magnesium alloys with ammoniated coating; (iii) bioactive drug: magnesium alloys with bioactive drug coating; and (iv) control: 0.9% NaCl.

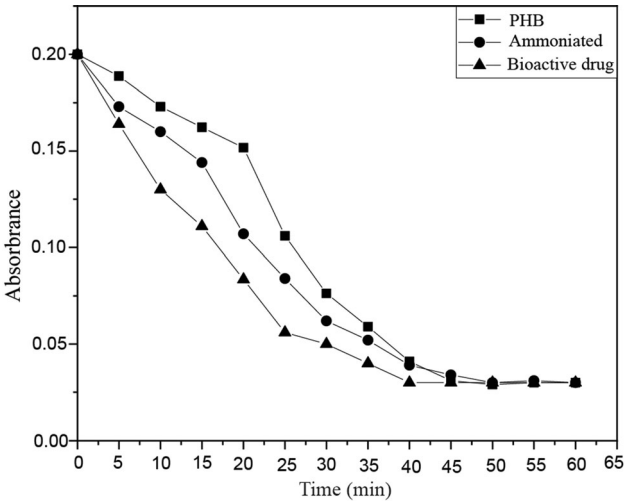

Figure 9 Dynamic clotting time of magnesium alloys with different coatings. (i) PHB: magnesium alloys with PHB coating; (ii) ammoniated: magnesium alloys with ammoniated coating; and (iii) bioactive drug: magnesium alloys with bioactive drug coating.

Dynamic clotting time

After materials contact with blood, dynamic clotting time can be used to test the extent of the intrinsic clotting factors and show effects of the materials on the blood coagulation time [39]. Absorbance was inversely proportional to the blood clotting time. Figure 9 shows that absorbance of the samples with bioactive drug coating was slower than other samples. It could be seen that the clotting time of samples with bioactive drug coating was longer than those of other samples. It indicated that bioactive drug possessed better anti-thrombin properties.

Cells adhesion morphology

As shown in Fig. 10, when the amount of HUVECs was fewer, cells were flattened and well spread across the surface and adhered to the substrate with cellular microextensions. After the cells covered microslide, cells contacted with neighbouring cells through short cell processes in a zipper-like manner. The samples with bioactive drug coating obviously had more cells on the microslide than control samples. The amount of cells increased with the concentration of extract. However, for other samples, the amount of adhesive cells on the microslide decreased with extract concentration. In Wang's research, surface modification using bioactive drug coating composed of heparin and VEGF could promote reendothelialization [40]. The different concentrations of the extracts of the magnesium alloys with bioactive drug coating could significantly increase the cell adhesion, which was a positive indicator to the cytocompatibility [22].

Cytoskeleton morphology

Figure 11 shows the cytoskeleton morphology after the 25%, 50% and 100% concentrations of the materials extracts incubating with cells for certain time. The morphology differences of the samples were counted and are shown in Fig. 12a–d. The cell staining with phalloidin could reflect the effects of the materials on the cells [41, 42]. Comparing the cell morphology and size after staining with phalloidin, it was found that cell aspect ratio and fluorescence intensity were not much different from the control samples. All samples had no obvious influences on the morphology of the cells. The cell area of the samples with bioactive drug coating was larger than other groups, which was probably because the drug promoted the growth of the cell.

AO/EB staining kit test

Figure 13 shows the image of HUVECs after AO/EB staining. The differences of samples are calculated in Fig. 14, and the ratios of living cells to dead cells of

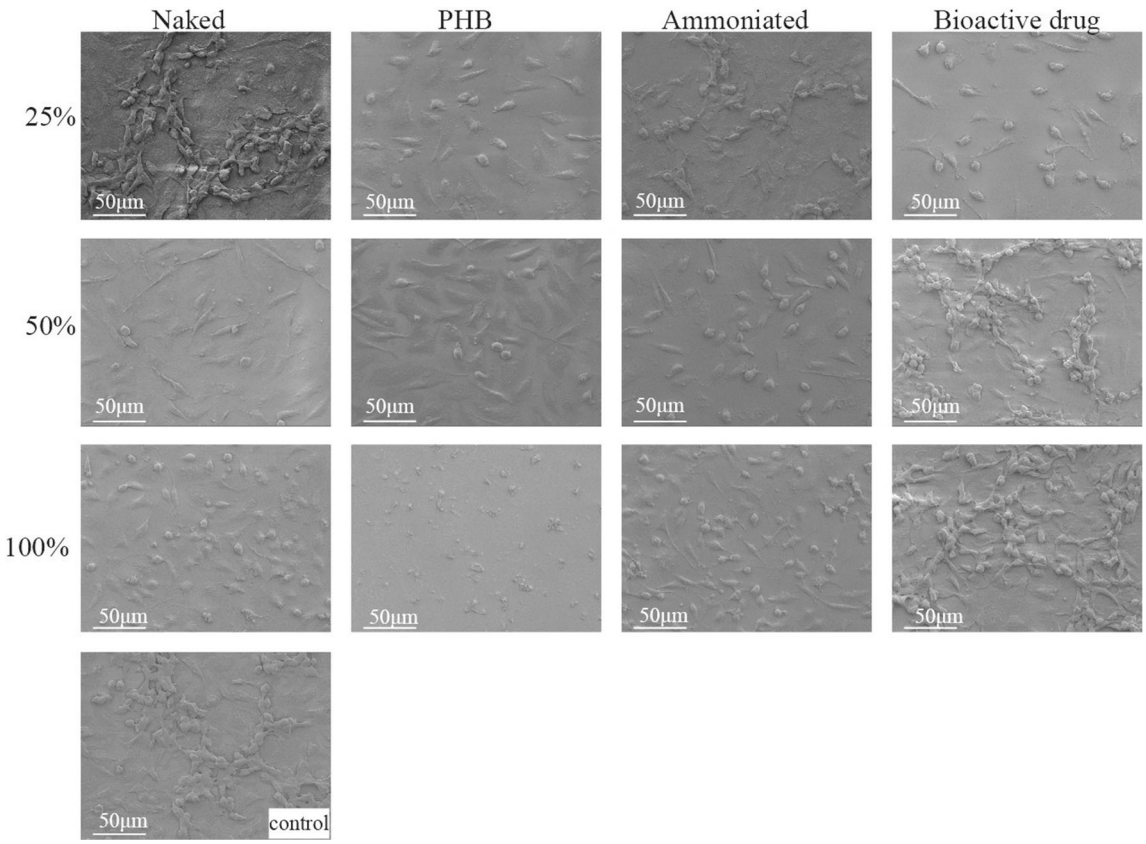

Figure 10 Microscopy images of HUVECs adhesion by SEM. (i) Naked: naked magnesium alloys; (ii) PHB: magnesium alloys with PHB coating; (iii) ammoniated: magnesium alloys with ammoniated coating; (iv) bioactive drug: magnesium alloys with bioactive drug coating; and (v) control: normal cultured cells. Original magnification: 500 ×.

the samples with bioactive drug coating and the samples with PHB coating were larger than that of the control group. These ratios of naked samples and ammoniated samples were smaller than that of the control group.

The ratio of living cells to apoptosis cells can be used to evaluate the effect of materials on cell injury [43, 44]. These results showed that the ratio was inversely proportional to the degree of cell injury. Therefore, the samples with bioactive drug coating and PHB coating could reduce cell apoptosis.

Conclusion

In this study, blood compatibility and cell compatibility were used to evaluate the biocompatibility of coated magnesium alloys. It is well known that heparin has a good anticoagulant effect and can effectively reduce the possibility of thrombosis [45, 46]. The hemolysis rate and platelet adhesion of the magnesium alloys with bioactive drug coating were much lower than magnesium alloys with other coatings, and the anti-thrombotic effect was also better. In addition, the magnesium alloys with bioactive drug coating greatly prolonged PT and APTT and prevented clotting on the surface of the materials. VEGF is a major driver of angiogenesis and vascular permeability of VEGF receptor 2 (VEGFR2), which can improve the biocompatibility of the sample surface with HUVEC and accelerate endothelialization [47, 48]. In this research, these magnesium alloys with bioactive drug did not change the morphology of the HUVECs, but increased cells growth. The results of AO/EB staining showed that the magnesium alloys with bioactive drug coating

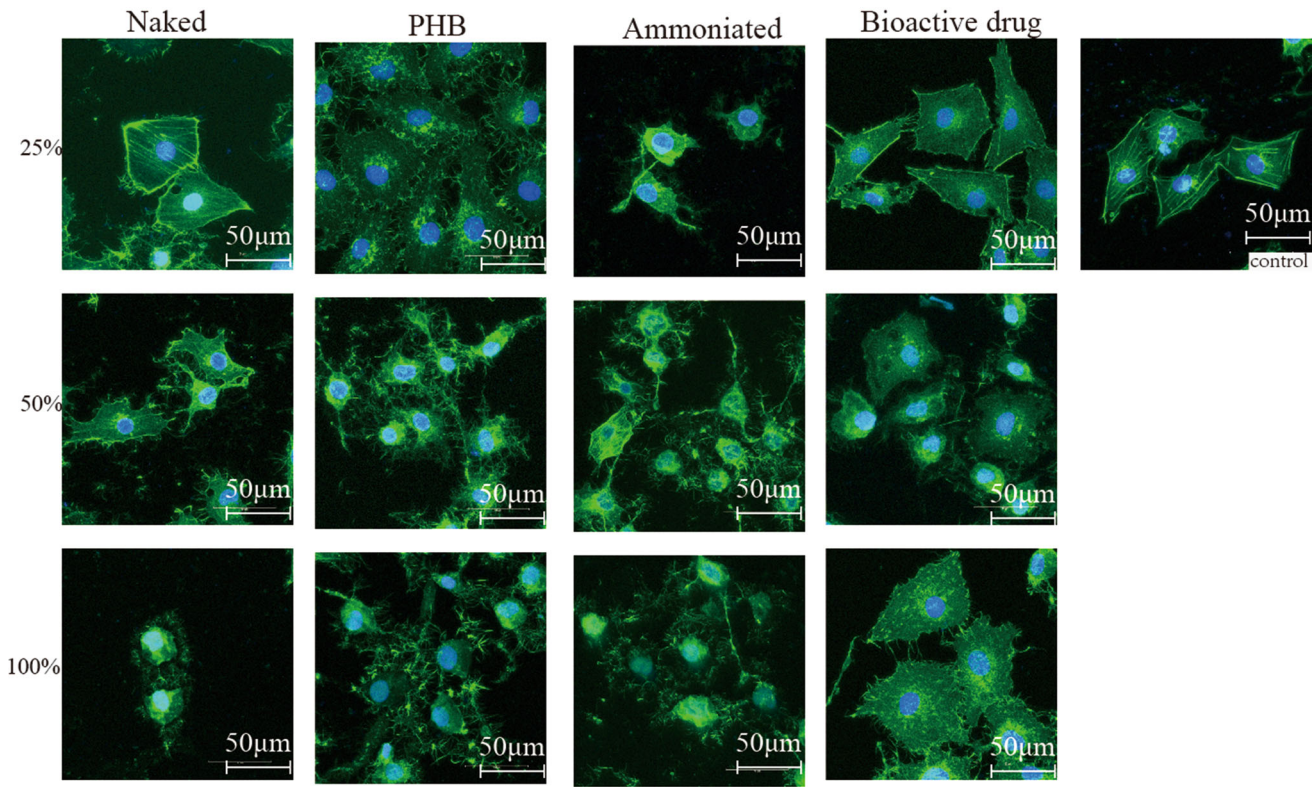

Figure 11 Cytoskeleton morphology of HUVECs after incubation with different concentrations of the materials extracts (25%, 50% and 100%). (i) Naked: naked magnesium alloys; (ii) PHB: magnesium alloys with PHB coating; (iii) ammoniated: magnesium alloys with ammoniated coating; (iv) bioactive drug: magnesium alloys with bioactive drug coating; and (v) control: normal cultured cells. Actin-Tracker Green showing the distribution of the microfilament skeleton in the cells; blue DAPI showing the morphology of the nucleus.

inhibited apoptosis to some extent. It indicates that VEGF and heparin can be assembled on the surface of the PHB coating by LbL self-assembly technique and maintain biological activity, which has improved significantly the biocompatibility of magnesium alloys. Some researchers also developed heparin/poly-L-Lysine nanoparticles and heparin-LDH/PDA as vascular stent coating. These strategies could improve the biocompatibility of materials, but slightly suppressed cell proliferation and decreased corrosion resistance [49, 50]. Bioactive drug coating adversely affected the biocompatibility of the substrate coating.

At present, researchers have done a lot of research on corrosion resistance and improving biocompatibility. However, these researches have not yet been clearly and effectively applied in clinical practice. There are still many problems in the development of new surface modification methods. Heparin and VEGF were used as coating drugs on magnesium

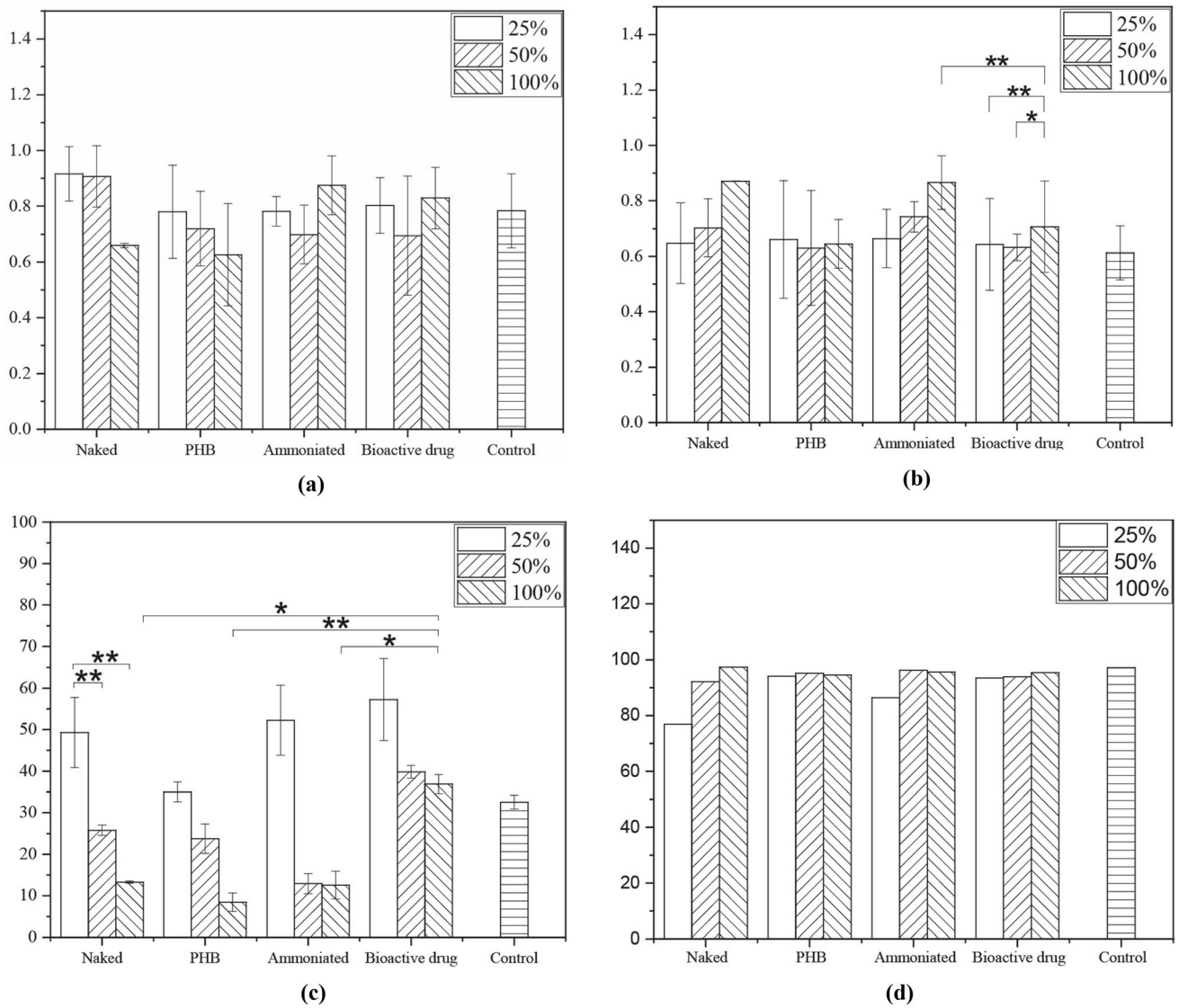

Figure 12 **a** Nucleus aspect ratio, **b** cell aspect ratio, **c** cell area, **d** fluorescence intensity.

alloy surface, which could achieve the dual effects of anti-thrombosis and promote endothelialization. The results will provide a new strategy for controllable degradation of magnesium alloys, which can contribute more to human health. In the future, the drug release behaviour and further research still need to provide more theoretical basis for the clinical application of these materials.

Acknowledgements

This work was partially supported by the NSFC 31700826. This work was also financially supported by Chongqing Research Program of Basic Research and Frontier Technology (cstc2017jcyjAX0284) and the Visiting Scholar Foundation of Key Laboratory of Biorheological Science and Technology

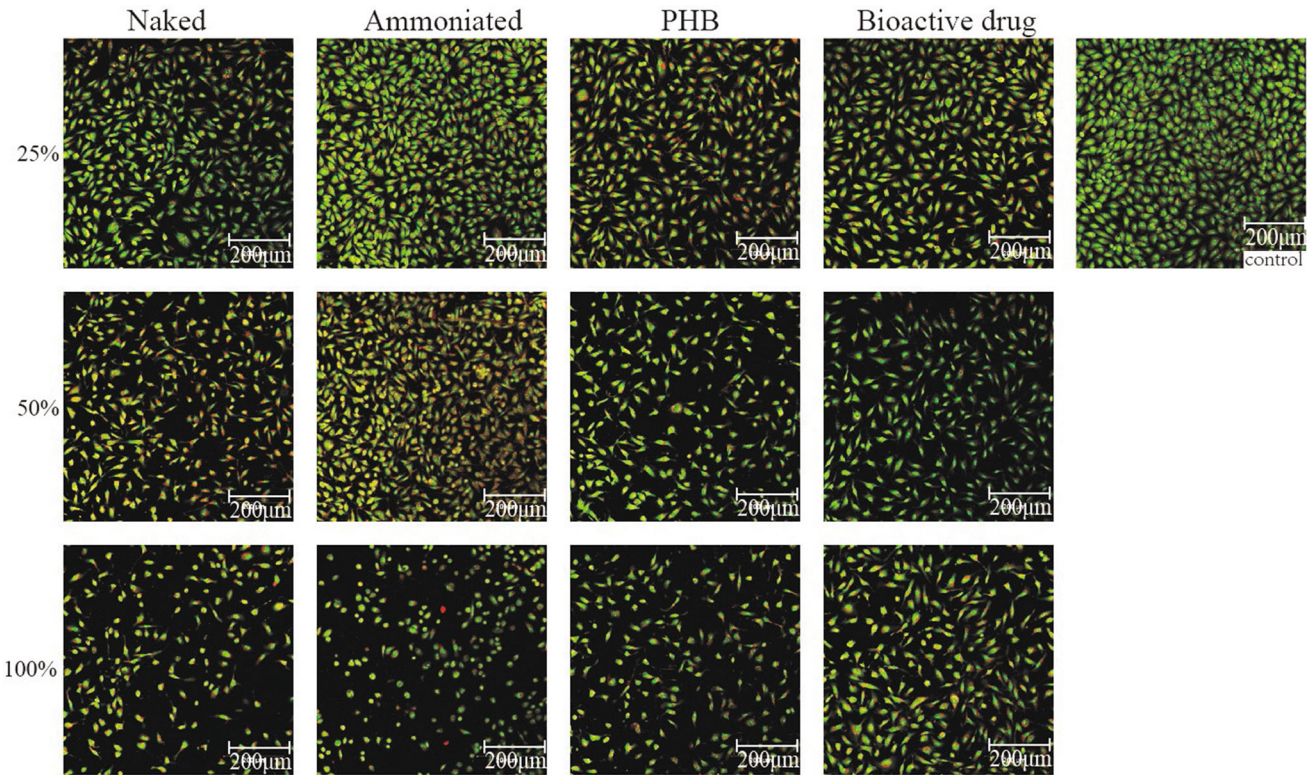

Figure 13 Cell apoptosis morphology after AO/EB staining by SEM. (i) Naked: naked magnesium alloys; (ii) PHB: magnesium alloys with PHB coating; (iii) ammoniated: magnesium alloys with ammoniated coating; (iv) bioactive drug: magnesium alloys with bioactive drug coating, and (v) control: normal cultured cells. AO emitting green fluorescence through cells with intact membranes; EB emitting orange–red fluorescence through cells damaged by membrane.

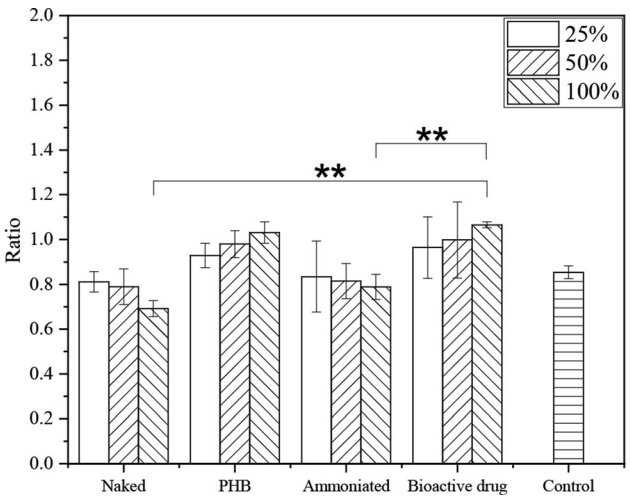

Figure 14 Ratio of living cells to dead cells after AO/EB staining. (i) Naked: naked magnesium alloys; (ii) PHB: magnesium alloys with PHB coating; (iii) ammoniated: magnesium alloys with ammoniated coating; (iv) bioactive drug: magnesium alloys with bioactive drug coating; and (v) control: normal cultured cells.

(Chongqing University), Ministry of Education (CQKLBST-2016-001).

References

[1] Abdal-hay A, Dewidar M, Lim J, Lim JK (2014) Ceram Int 40:2237. https://doi.org/10.1016/j.ceramint.2013.07.142

[2] Abdal-hay A, Amna T, Lim JK (2013) Solid State Sci 18:131. https://doi.org/10.1016/j.solidstatesciences.2012.11.017

[3] Adhikari U, Rijal NP, Khanal S, Pai D, Sankar J, Bhattarai N (2016) Bioact Mater 1:132. https://doi.org/10.1016/j.bioactmat.2016.11.003

[4] Agarwal S, Curtin J, Duffy B, Jaiswal S (2016) Mater Sci Eng C-Mater Biol Appl 68:948. https://doi.org/10.1016/j.msec.2016.06.020

[5] Chen J, Tan L, Yu X, Etim IP, Ibrahim M, Yang K (2018) J Mech Behav Biomed Mater 87:68. https://doi.org/10.1016/j.jmbbm.2018.07.022

[6] Echeverry-Rendon M, Allain JP, Robledo SM, Echeverria F, Harmsen MC (2019) Mater Sci Eng C-Mater Biol Appl 102:150. https://doi.org/10.1016/j.msec.2019.04.032
[7] Argarate N, Olalde B, Atorrasagasti G et al (2014) Mater Lett 132:193. https://doi.org/10.1016/j.matlet.2014.06.070
[8] Bakhsheshi-Rad HR, Hamzah E, Kasiri-Asgarani M, Jabbarzare S, Iqbal N, Kadir MRA (2016) Mater Sci Eng C-Mater Biol Appl 60:526. https://doi.org/10.1016/j.msec.2015.11.057
[9] Cordoba LC, Marques A, Taryba M, Coradin T, Montemor F (2018) Surf Coat Technol 341:103. https://doi.org/10.1016/j.surfcoat.2017.08.062
[10] Cui LY, Fang XH, Cao W et al (2018) Appl Surf Sci 457:49. https://doi.org/10.1016/j.apsusc.2018.06.240
[11] Celarek A, Kraus T, Tschegg EK et al (2012) Mater Sci Eng C-Mater Biol Appl 32:1503. https://doi.org/10.1016/j.msec.2012.04.032
[12] Miller ND, Williams DF (1987) Biomaterials 8:129. https://doi.org/10.1016/0142-9612(87)90102-5
[13] Raza ZA, Riaz S, Banat IM (2018) Biotechnol Prog 34:29. https://doi.org/10.1002/btpr.2565
[14] Jin S, Gu H, Chen XS et al (2018) Colloid Surf. B-Biointerfaces 167:28. https://doi.org/10.1016/j.colsurfb.2018.03.047
[15] Zhao Q, Mahmood W, Zhu YY (2016) Appl Surf Sci 367:249. https://doi.org/10.1016/j.apsusc.2016.01.055
[16] Ruttala HB, Ramasamy T, Shin BS, Choi HG, Yong CS, Kim JO (2017) Int J Pharm 519:11. https://doi.org/10.1016/j.ijpharm.2017.01.011
[17] Abdelwahab MA, El-Barbary AA, El-Said KS, El Naggar SA, ElKholy HM (2019) Int J Biol Macromol 122:793. https://doi.org/10.1016/j.ijbiomac.2018.10.164
[18] Yang H, Qu X, Lin W, Wang C et al (2018) Acta Biomater 71:200–214
[19] Gu X, Zheng Y, Cheng Y et al (2009) Biomaterials 30:484
[20] Lee JY, Schmidt C (2015) J Biomed Mater Res Part A 103:2126
[21] Venault A, Hsu K-J, Yeh L-C et al (2017) Colloids Surf B Biointerfaces 151:372
[22] Chen HY, Zhang EL, Yang K (2014) Mater Sci Eng C-Mater Biol Appl 34:201. https://doi.org/10.1016/j.msec.2013.09.010
[23] Goosen MFA, Sefton MV (1983) J Biomed Mater Res 17:359
[24] Liu Y, Zhang J, Wang J et al (2015) J Biomed Mater Res Part A 103:2024. https://doi.org/10.1002/jbm.a.35339
[25] Zhu S-J, Liu Q, Qian Y-F et al (2014) Front Mater Sci 8:256. https://doi.org/10.1007/s11706-014-0259-3
[26] Zou YH, Zeng RC, Wang QZ et al (2016) Front Mater Sci 10:281. https://doi.org/10.1007/s11706-016-0345-9
[27] Riaz A, Khan RA, Mirza T, Mustansir T, Ahmed M (2014) Pak J Pharm Sci 27:907
[28] Lehle K, Gessner A, Wehner D, Schmid T, Wendel HP, Schmid C (2015) Transpl Int 28:42
[29] Lin WC, Liu TY, Yang MCJB (2004) Biomaterials 25:1947
[30] McDonald SM, Matheson LA, McBane JE et al (2011) J Cell Biochem 112:3762. https://doi.org/10.1002/jcb.23307
[31] McBane JE, Ebadi D, Sharifpoor S, Labow RS, Santerre JP (2011) Acta Biomater 7:115. https://doi.org/10.1016/j.actbio.2010.08.014
[32] McGuigan AP, Sefton MV (2007) Biomaterials 28:2547. https://doi.org/10.1016/j.biomaterials.2007.01.039
[33] McBane JE, Matheson LA, Sharifpoor S, Santerre JP, Labow RS (2009) Biomaterials 30:5497. https://doi.org/10.1016/j.biomaterials.2009.07.010
[34] Brockman KS, Kizhakkedathu JN, Santerre JP (2017) Acta Biomater 48:368. https://doi.org/10.1016/j.actbio.2016.11.005
[35] Zhang XY, Zhang GN, Zhang HY, Li JF, Yao XH, Tang B (2018) Colloid Surf B-Biointerfaces 172:338. https://doi.org/10.1016/j.colsurfb.2018.08.060
[36] Sadowski R, Gadzala-Kopciuch R, Buszewski B (2019) Curr Med Chem 26:166. https://doi.org/10.2174/0929867324666171005114150
[37] Khanna V, Shahzad A, Thayalasamy K et al (2018) Thromb Res 172:36. https://doi.org/10.1016/j.thromres.2018.09.062
[38] Dunne E, O'Halloran M, Porter E et al (2019) IEEE Trans Dielectr Electr Insul 26:229. https://doi.org/10.1109/tdei.2018.007508
[39] Yuan Y, Liu C, Yin M (2008) J Mater Sci-Mater Med 19:2187. https://doi.org/10.1007/s10856-007-3319-8
[40] Wang HG, Yin TY, Ge SP et al (2013) J Biomed Mater Res Part A 101:413. https://doi.org/10.1002/jbm.a.34339
[41] Ledda M, De Bonis A, Bertani FR et al (2015) Biomed Mater 10:7. https://doi.org/10.1088/1748-6041/10/3/035005
[42] Lin X, Tan L, Wang Q, Zhang G, Zhang B, Yang K (2013) Mater Sci Eng C-Mater Biol Appl 33:3881. https://doi.org/10.1016/j.msec.2013.05.023
[43] Nasiri M, Hassanzadeh-Tabrizi SA (2018) J Chin Chem Soc 65:231. https://doi.org/10.1002/jccs.201700271
[44] Tanasie G, Bojin F, Tatu RF et al (2017) Mater Plast 54:523
[45] Barrowcliffe TW (2012) In: Lever R, Mulloy B, Page CP (eds) Heparin - A century of progress. Handbook of experimental pharmacology, vol 207. Springer, Berlin, Heidelberg
[46] Onishi A, St Ange K, Dordick JS, Linhardt RJ (2016) Front Biosci 21:1372
[47] Zhang H, Jia X, Han F et al (2013) Biomaterials 34:2202
[48] Heinolainen K, Karaman S, Amico GD et al (2017) Circ Res J Am Heart 120:1414

[49] Li H, Peng F, Wang D, Qiao Y, Xu D, Liu X (2018) Biomater Sci 6:1846
[50] Liu T, Zeng Z, Liu Y et al (2014) ACS Appl Mater Interfaces 6:8729. https://doi.org/10.1021/am5015309